

Measurement of matter–antimatter differences in beauty baryon decays

The LHCb collaboration[†]

Differences in the behaviour of matter and antimatter have been observed in K and B meson decays, but not yet in any baryon decay. Such differences are associated with the non-invariance of fundamental interactions under the combined charge-conjugation and parity transformations, known as CP violation. Here, using data from the LHCb experiment at the Large Hadron Collider, we search for CP -violating asymmetries in the decay angle distributions of Λ_b^0 baryons decaying to $p\pi^-\pi^+\pi^-$ and $p\pi^-K^+K^-$ final states. These four-body hadronic decays are a promising place to search for sources of CP violation both within and beyond the standard model of particle physics. We find evidence for CP violation in Λ_b^0 to $p\pi^-\pi^+\pi^-$ decays with a statistical significance corresponding to 3.3 standard deviations including systematic uncertainties. This represents the first evidence for CP violation in the baryon sector.

The asymmetry between matter and antimatter is related to the violation of the CP symmetry (CPV), where C and P are the charge-conjugation and parity operators. CP violation is accommodated in the standard model (SM) of particle physics by the Cabibbo–Kobayashi–Maskawa (CKM) mechanism that describes the transitions between up- and down-type quarks^{1,2}, in which quark decays proceed by the emission of a virtual W boson and where the phases of the couplings change sign between quarks and antiquarks. However, the amount of CPV predicted by the CKM mechanism is not sufficient to explain our matter-dominated Universe^{3,4} and other sources of CPV are expected to exist. The initial discovery of CPV was in neutral K meson decays⁵, and more recently it has been observed in B^0 (refs 6,7), B^+ (refs 8–11), and B_s^0 (ref. 12) meson decays, but it has never been observed in the decays of any baryon. Decays of the Λ_b^0 (*bud*) baryon to final states consisting of hadrons with no charm quarks are predicted to have non-negligible CP asymmetries in the SM, as large as 20% for certain three-body decay modes¹³. It is important to measure the size and nature of these CP asymmetries in as many decay modes as possible, to determine whether they are consistent with the CKM mechanism or, if not, what extensions to the SM would be required to explain them^{14–16}.

The decay processes studied in this article, $\Lambda_b^0 \rightarrow p\pi^-\pi^+\pi^-$ and $\Lambda_b^0 \rightarrow p\pi^-K^+K^-$, are mediated by the weak interaction and governed mainly by two amplitudes, expected to be of similar magnitude, from different diagrams describing quark-level $b \rightarrow u\bar{u}d$ transitions, as shown in Fig. 1. Throughout this paper the inclusion of charge-conjugate reactions is implied, unless otherwise indicated. CPV could arise from the interference of two amplitudes with relative phases that differ between particle and antiparticle decays, leading to differences in the Λ_b^0 and $\bar{\Lambda}_b^0$ decay rates. The main source of this effect in the SM would be the large relative phase (referred to as α in the literature) between the product of the CKM matrix elements $V_{ub}V_{ud}^*$ and $V_{cb}V_{cd}^*$, which are present in the different diagrams depicted in Fig. 1. Parity violation (PV) is also expected in weak interactions, but has never been observed in Λ_b^0 decays.

To search for CP -violating effects one needs to measure CP -odd observables, which can be done by studying asymmetries in the \hat{T} operator. This is a unitary operator that reverses both the momentum and spin three-vectors^{17,18}, and is different from the antiunitary time-reversal operator T ^{19,20} that also exchanges

initial and final states. A non-zero CP -odd observable implies CP violation, and similar considerations apply to P -odd observables and parity violation²¹. Furthermore, different values of P -odd observables for a decay and its charge conjugate would imply CPV. In this paper, scalar triple products of final-state particle momenta in the Λ_b^0 centre-of-mass frame are studied to search for P - and CP -violating effects in four-body decays. These are defined as $C_{\hat{T}} = \mathbf{p}_p \cdot (\mathbf{p}_{h_1^-} \times \mathbf{p}_{h_2^+})$ for Λ_b^0 and $\bar{C}_{\hat{T}} = \mathbf{p}_{\bar{p}} \cdot (\mathbf{p}_{h_1^+} \times \mathbf{p}_{h_2^-})$ for $\bar{\Lambda}_b^0$, where h_1 and h_2 are final-state hadrons: $h_1 = \pi$ and $h_2 = K$ for $\Lambda_b^0 \rightarrow p\pi^-K^+K^-$ and $h_1 = h_2 = \pi$ for $\Lambda_b^0 \rightarrow p\pi^-\pi^+\pi^-$. In the latter case there is an inherent ambiguity in the choice of the pion for h_1 that is resolved by taking that with the larger momentum in the Λ_b^0 rest frame, referred to as π_{fast} . The following asymmetries may then be defined^{22,23}:

$$A_{\hat{T}}(C_{\hat{T}}) = \frac{N(C_{\hat{T}} > 0) - N(C_{\hat{T}} < 0)}{N(C_{\hat{T}} > 0) + N(C_{\hat{T}} < 0)} \quad (1)$$

$$\bar{A}_{\hat{T}}(\bar{C}_{\hat{T}}) = \frac{\bar{N}(-\bar{C}_{\hat{T}} > 0) - \bar{N}(-\bar{C}_{\hat{T}} < 0)}{\bar{N}(-\bar{C}_{\hat{T}} > 0) + \bar{N}(-\bar{C}_{\hat{T}} < 0)} \quad (2)$$

where N and \bar{N} are the numbers of Λ_b^0 and $\bar{\Lambda}_b^0$ decays. These asymmetries are P -odd and \hat{T} -odd and so change sign under P or \hat{T} transformations, that is, $A_{\hat{T}}(C_{\hat{T}}) = -A_{\hat{T}}(-C_{\hat{T}})$ or $\bar{A}_{\hat{T}}(\bar{C}_{\hat{T}}) = -\bar{A}_{\hat{T}}(-\bar{C}_{\hat{T}})$. The P - and CP -violating observables are defined as

$$a_P^{\hat{T}\text{-odd}} = \frac{1}{2}(A_{\hat{T}} + \bar{A}_{\hat{T}}), \quad a_{CP}^{\hat{T}\text{-odd}} = \frac{1}{2}(A_{\hat{T}} - \bar{A}_{\hat{T}}) \quad (3)$$

and a significant deviation from zero would signal PV or CPV, respectively.

Searches for CPV with triple-product asymmetries are particularly suited to Λ_b^0 four-body decays to hadrons with no charm quark²⁴ thanks to the rich resonant substructure, dominated by $\Delta(1232)^{++} \rightarrow p\pi^+$ and $\rho(770)^0 \rightarrow \pi^+\pi^-$ resonances in the $\Lambda_b^0 \rightarrow p\pi^-\pi^+\pi^-$ final state. The observable $a_{CP}^{\hat{T}\text{-odd}}$ is sensitive to the interference of \hat{T} -even and \hat{T} -odd amplitudes with different CP -odd ('weak') phases. Unlike the overall asymmetry in the decay rate that is sensitive to the interference of \hat{T} -even amplitudes, $a_{CP}^{\hat{T}\text{-odd}}$ does not require a non-vanishing difference

[†]A full list of authors and affiliations appears at the end of the paper.

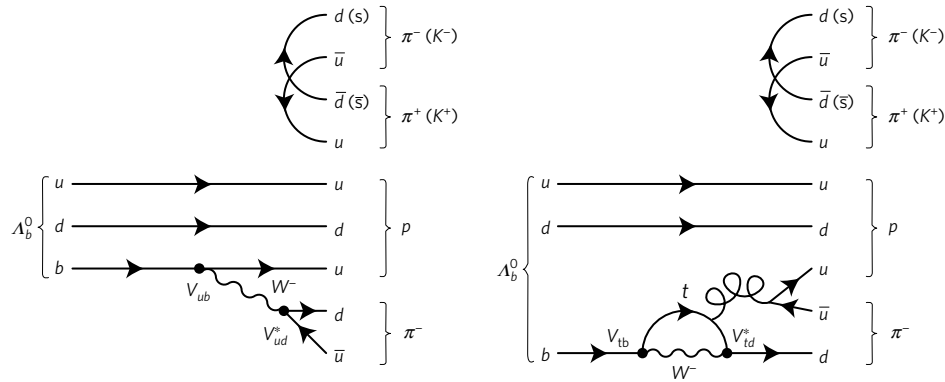


Figure 1 | Dominant Feynman diagrams for $\Lambda_b^0 \rightarrow p\pi^-\pi^+\pi^-$ and $\Lambda_b^0 \rightarrow p\pi^-K^+K^-$ transitions. The two diagrams show the transitions that contribute most strongly to $\Lambda_b^0 \rightarrow p\pi^-\pi^+\pi^-$ and $\Lambda_b^0 \rightarrow p\pi^-K^+K^-$ decays. In both cases, a pair of $\pi^+\pi^-$ (K^+K^-) is produced by gluon emission from the light quarks (u,d). The difference is in the b quark decay that happens on the left through a virtual W^- boson emission ('tree diagram') and on the right as a virtual W^- boson emission and absorption together with a gluon emission ('loop diagram'). The magnitudes of the two amplitudes are expected to be comparable, and each is proportional to the product of the CKM matrix elements involved, which are shown in the figure.

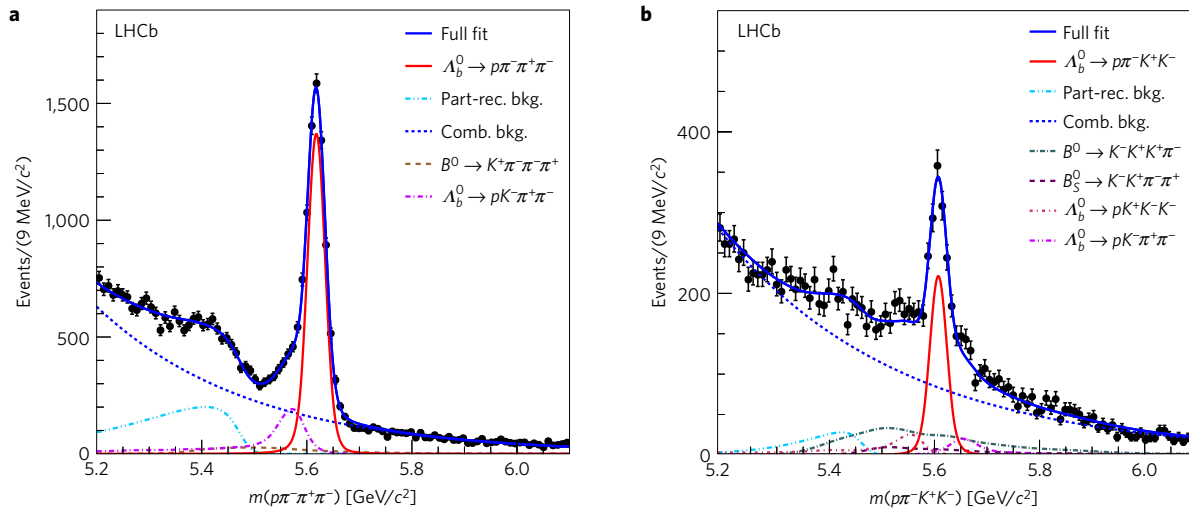


Figure 2 | Reconstructed invariant mass fits used to extract the signal yields. The invariant mass distributions for (a) $\Lambda_b^0 \rightarrow p\pi^-\pi^+\pi^-$ and (b) $\Lambda_b^0 \rightarrow p\pi^-K^+K^-$ decays are shown. A fit is overlaid on top of the data points, with solid and dotted lines describing the projections of the fit results for each of the components described in the text and listed in the legend. Uncertainties on the data points are statistical only and represent one standard deviation, calculated assuming Poisson-distributed entries.

in the CP -invariant ('strong') phase between the contributing amplitudes^{19,25}. The observables $A_{\overline{T}}$, $\overline{A}_{\overline{T}}$, $a_p^{\overline{T}\text{-odd}}$ and $a_{CP}^{\overline{T}\text{-odd}}$ are, by construction, largely insensitive to particle–antiparticle production asymmetries and detector-induced charge asymmetries²⁶.

This article describes measurements of the CP - and P -violating asymmetries introduced in equation (3) in $\Lambda_b^0 \rightarrow p\pi^-\pi^+\pi^-$ and $\Lambda_b^0 \rightarrow p\pi^-K^+K^-$ decays. The asymmetries are measured first for the entire phase space of the decay, integrating over all possible final-state configurations, and then in different regions of phase space so as to enhance sensitivity to localized CPV. The analysis is performed using proton–proton collision data collected by the LHCb detector, corresponding to 3.0 fb^{-1} of integrated luminosity at centre-of-mass energies of 7 and 8 TeV, and exploits the copious production of Λ_b^0 baryons at the LHC, which constitutes around 20% of all b hadrons produced²⁷. Control samples of $\Lambda_b^0 \rightarrow pK^-\pi^+\pi^-$ and $\Lambda_b^0 \rightarrow \Lambda_c^+\pi^-$ decays, with Λ_c^+ decaying to $pK^-\pi^+$, $p\pi^-\pi^+$, and pK^-K^+ final states, are used to optimize the event selection and study systematic effects; the most abundant control sample consists of $\Lambda_b^0 \rightarrow \Lambda_c^+(pK^-\pi^+)\pi^-$ decays mediated by $b \rightarrow c$ quark transitions in which no CPV is expected²⁸. To avoid introducing biases in the results, all aspects of the analysis, including the

selection, phase space regions, and procedure used to determine the statistical significance of the results, were fixed before the data were examined.

The LHCb detector^{29,30} is designed to collect data of b -hadron decays produced from proton–proton collisions at the Large Hadron Collider. It instruments a region around the proton beam axis, covering the polar angles between 10 and 250 mrad, where approximately 24% of the b -hadron decays occur³¹. The detector includes a high-precision tracking system with a dipole magnet, providing measurements of the momentum and decay vertex position of particle decays. Different types of charged particles are distinguished using information from two ring-imaging Cherenkov detectors, a calorimeter and a muon system. Simulated samples of Λ_b^0 signal modes and control samples are used in this analysis to verify the experimental method and to study certain systematic effects. These simulated events model the experimental conditions in detail, including the proton–proton collision, the decays of the particles, and the response of the detector. The software used is described in refs 32–38. The online event selection is performed by a trigger system that takes fast decisions about which events to record. It consists of a hardware stage, based on information from the

Table 1 | Definition of binning scheme A for the decay mode $\Lambda_b^0 \rightarrow p\pi^-\pi^+\pi^-$.

Phase space bin	$m(p\pi^+)$	$m(p\pi_{\text{slow}}^-)$	$m(\pi^+\pi_{\text{slow}}^-), m(\pi^+\pi_{\text{fast}}^-)$	$ \Phi $
1	(1.07,1.23)			$(0, \frac{\pi}{2})$
2	(1.07,1.23)			$(\frac{\pi}{2}, \pi)$
3	(1.23,1.35)			$(0, \frac{\pi}{2})$
4	(1.23,1.35)			$(\frac{\pi}{2}, \pi)$
5	(1.35, 5.34)	(1.07, 2.00)	$m(\pi^+\pi_{\text{slow}}^-) < 0.78$ or $m(\pi^+\pi_{\text{fast}}^-) < 0.78$	$(0, \frac{\pi}{2})$
6	(1.35, 5.34)	(1.07, 2.00)	$m(\pi^+\pi_{\text{slow}}^-) < 0.78$ or $m(\pi^+\pi_{\text{fast}}^-) < 0.78$	$(\frac{\pi}{2}, \pi)$
7	(1.35, 5.34)	(1.07, 2.00)	$m(\pi^+\pi_{\text{slow}}^-) > 0.78$ and $m(\pi^+\pi_{\text{fast}}^-) > 0.78$	$(0, \frac{\pi}{2})$
8	(1.35, 5.34)	(1.07, 2.00)	$m(\pi^+\pi_{\text{slow}}^-) > 0.78$ and $m(\pi^+\pi_{\text{fast}}^-) > 0.78$	$(\frac{\pi}{2}, \pi)$
9	(1.35, 5.34)	(2.00, 4.00)	$m(\pi^+\pi_{\text{slow}}^-) < 0.78$ or $m(\pi^+\pi_{\text{fast}}^-) < 0.78$	$(0, \frac{\pi}{2})$
10	(1.35, 5.34)	(2.00, 4.00)	$m(\pi^+\pi_{\text{slow}}^-) < 0.78$ or $m(\pi^+\pi_{\text{fast}}^-) < 0.78$	$(\frac{\pi}{2}, \pi)$
11	(1.35, 5.34)	(2.00, 4.00)	$m(\pi^+\pi_{\text{slow}}^-) > 0.78$ and $m(\pi^+\pi_{\text{fast}}^-) > 0.78$	$(0, \frac{\pi}{2})$
12	(1.35, 5.34)	(2.00, 4.00)	$m(\pi^+\pi_{\text{slow}}^-) > 0.78$ and $m(\pi^+\pi_{\text{fast}}^-) > 0.78$	$(\frac{\pi}{2}, \pi)$

Binning scheme A is defined to exploit interference patterns arising from the resonant structure of the decay. Bins 1-4 focus on the region dominated by the $\Delta(1232)^{++} \rightarrow p\pi^+$ resonance. The other eight bins are defined to study regions where $p\pi^-$ resonances are present (5-8) on either side of the $\rho(770)^0 \rightarrow \pi^+\pi^-$ resonances (5-12). Further splitting for $|\Phi|$ lower or greater than $\pi/2$ is done to reduce potential dilution of asymmetries, as suggested in ref. 19. Masses are in units of GeV/c^2 .

calorimeter and muon systems, followed by a software stage, which applies a full event reconstruction. The software trigger requires Λ_b^0 candidates to be consistent with a b -hadron decay topology, with tracks originating from a secondary vertex detached from the primary pp collision point. The mean Λ_b^0 lifetime is 1.5 ps (ref. 39), which corresponds to a typical flight distance of a few millimetres in the LHCb.

The $\Lambda_b^0 \rightarrow p\pi^-h^+h^-$ candidates are formed by combining tracks identified as protons, pions, or kaons that originate from a common vertex. The proton or antiproton identifies the candidate as a Λ_b^0 or $\bar{\Lambda}_b^0$. There are backgrounds from b -hadron decays to charm hadrons that are suppressed by reconstructing the appropriate two- or three-body invariant masses, and requiring them to differ from the known charm hadron masses by at least three times the experimental resolution. For the $\Lambda_b^0 \rightarrow \Lambda_c^+\pi^-$ control mode, only the $\Lambda_b^0 \rightarrow ph^+h^-\pi^-$ events with reconstructed ph^+h^- invariant mass between 2.23 and 2.31 GeV/c^2 are retained.

A boosted decision tree (BDT) classifier⁴⁰ is constructed from a set of kinematic variables that discriminate between signal and background. The signal and background training samples used for the BDT are derived from the $\Lambda_b^0 \rightarrow pK^-\pi^+\pi^-$ control sample, since its kinematics and topology are similar to the decays under study; background in this sample is subtracted with the *sPlot* technique⁴¹, a statistical technique to disentangle signal and background contributions. The background training sample consists of candidates that lie far from the signal mass peak, between 5.85 and 6.40 GeV/c^2 . The control modes $\Lambda_b^0 \rightarrow \Lambda_c^+(p\pi^+\pi^-)\pi^-$ and $\Lambda_b^0 \rightarrow \Lambda_c^+(pK^-K^+)\pi^-$ are used to optimize the particle identification criteria for the signal mode with the same final state. For events in which multiple candidates pass all selection criteria for a given mode, one candidate is retained at random and the rest discarded.

Unbinned extended maximum likelihood fits to the $p\pi^-\pi^+\pi^-$ and the $p\pi^-K^+K^-$ invariant mass distributions are shown in Fig. 2. The invariant mass distribution of the Λ_b^0 signal is modelled by a Gaussian core with power-law tails⁴², with the mean and the width of the Gaussian determined from the fit to data. The combinatorial background is modelled by an exponential distribution with the rate parameter extracted from data. All other parameters of the fit model are taken from simulations except the yields. Partially reconstructed Λ_b^0 decays are described by an empirical function⁴³ convolved with a Gaussian function to account for resolution effects. The shapes of backgrounds from other b -hadron decays due to incorrectly identified particles, for example, kaons identified as pions or protons identified as kaons, are modelled using simulated events. These

consist mainly of $\Lambda_b^0 \rightarrow pK^-\pi^+\pi^-$ and $B^0 \rightarrow K^+\pi^-\pi^-\pi^+$ decays for the $\Lambda_b^0 \rightarrow p\pi^-\pi^+\pi^-$ sample and of similar final states for the $\Lambda_b^0 \rightarrow p\pi^-K^+K^-$ sample, as shown in Fig. 2. The yields of these contributions are obtained from fits to data reconstructed under the appropriate mass hypotheses for the final-state particles. The signal yields of $\Lambda_b^0 \rightarrow p\pi^-\pi^+\pi^-$ and $\Lambda_b^0 \rightarrow p\pi^-K^+K^-$ are $6,646 \pm 105$ and $1,030 \pm 56$, respectively. This is the first observation of these decay modes.

Signal candidates are split into four categories according to Λ_b^0 or $\bar{\Lambda}_b^0$ flavour and the sign of $C_{\hat{\tau}}$ or $\bar{C}_{\hat{\tau}}$ to calculate the asymmetries defined in equations (1) and (2). The reconstruction efficiency for signal candidates with $C_{\hat{\tau}} > 0$ is identical to that with $C_{\hat{\tau}} < 0$ within the statistical uncertainties of the control sample, and likewise for $\bar{C}_{\hat{\tau}}$, which indicates that the detector and the reconstruction program do not bias this measurement. This check is performed both on the $\Lambda_b^0 \rightarrow \Lambda_c^+(pK^-\pi^+)\pi^-$ data control sample and on large samples of simulated events, using yields about 30 times those found in data, which are generated with no CP asymmetry. The CP asymmetry measured in the control sample is $a_{CP}^{\hat{\tau}\text{-odd}}(\Lambda_c^+\pi^-) = (0.15 \pm 0.31)\%$, compatible with CP symmetry. The asymmetries $A_{\hat{\tau}}$ and $\bar{A}_{\hat{\tau}}$ in the signal samples are measured with a simultaneous unbinned maximum likelihood fit to the invariant mass distributions of the different signal categories, and are found to be uncorrelated. Corresponding asymmetries for each of the background components are also measured in the fit; they are found to be consistent with zero, and do not lead to significant systematic uncertainties in the signal asymmetries. The values of $a_{CP}^{\hat{\tau}\text{-odd}}$ and $\bar{a}_{CP}^{\hat{\tau}\text{-odd}}$ are then calculated from $A_{\hat{\tau}}$ and $\bar{A}_{\hat{\tau}}$.

In four-body particle decays, the CP asymmetries may vary over

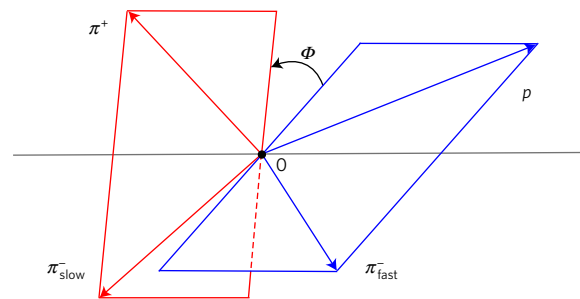


Figure 3 | Definition of the Φ angle. The decay planes formed by the $p\pi_{\text{fast}}^-$ (blue) and the $\pi_{\text{slow}}^-\pi^+$ (red) systems in the Λ_b^0 rest frame. The momenta of the particles, represented by vectors, determine the two decay planes and the angle $\Phi \in [-\pi, \pi]$ (ref. 19) measures their relative orientation.

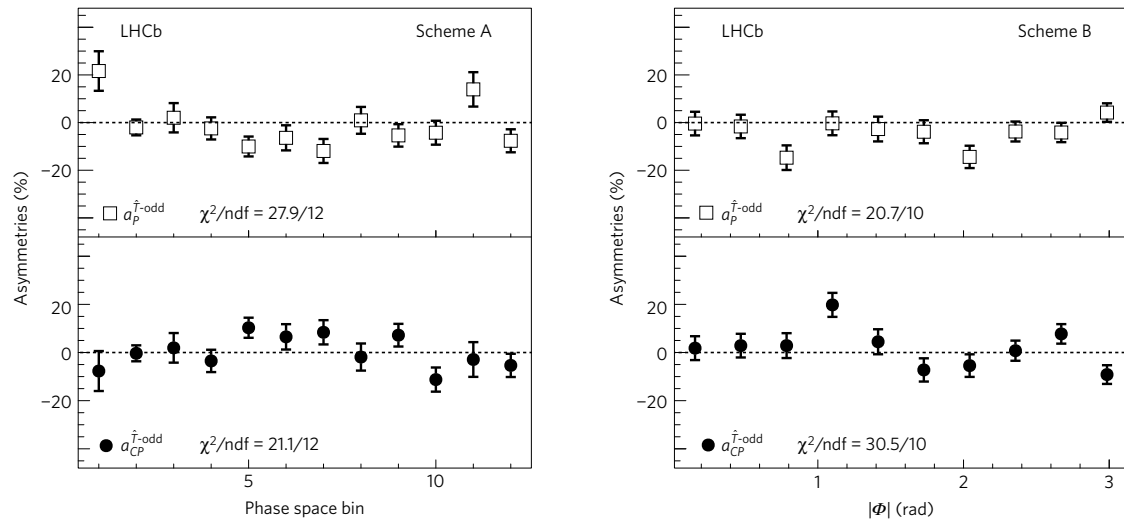


Figure 4 | Distributions of the asymmetries. The results of the fit in each region of binning schemes A and B are shown. The asymmetries $a_p^{\tilde{T}\text{-odd}}$ and $a_{CP}^{\tilde{T}\text{-odd}}$ for $\Lambda_b^0 \rightarrow p\pi^-\pi^+\pi^-$ decays are represented by open boxes and filled circles, respectively. The error bars represent one standard deviation, calculated as the sum in quadrature of the statistical uncertainty resulting from the fit to the invariant mass distribution and the systematic uncertainties estimated as described in the main text. The values of the χ^2/ndf are quoted for the P - and CP -conserving hypotheses for each binning scheme, where ndf indicates the number of degrees of freedom.

the phase space due to resonant contributions or their interference effects, possibly cancelling when integrated over the whole phase space. Therefore, the asymmetries are measured in different regions of phase space for the $\Lambda_b^0 \rightarrow p\pi^-\pi^+\pi^-$ decay using two binning schemes, defined before examining the data. Scheme A, defined in Table 1, is designed to isolate regions of phase space according to their dominant resonant contributions. Scheme B exploits in more detail the interference of contributions which could be visible as a function of the angle Φ between the decay planes formed by the $p\pi_{\text{fast}}^-$ and the $\pi_{\text{slow}}^-\pi^+$ systems, as illustrated in Fig. 3. Scheme B has ten non-overlapping bins of width $\pi/10$ in $|\Phi|$. For every bin in each of the schemes, the Λ_b^0 efficiencies for $C_{\tilde{T}} > 0$ and $C_{\tilde{T}} < 0$ are compared and found to be equal within uncertainties, and likewise the $\bar{\Lambda}_b^0$ efficiencies for $\bar{C}_{\tilde{T}} > 0$ and $\bar{C}_{\tilde{T}} < 0$. The analysis technique is validated on the $\Lambda_b^0 \rightarrow \Lambda_c^+(pK^-\pi^+)\pi^-$ control sample, for which the angle Φ is defined by the decay planes of the pK^- and $\pi^+\pi^-$ pairs, and on simulated signal events.

The asymmetries measured in $\Lambda_b^0 \rightarrow p\pi^-\pi^+\pi^-$ decays with these two binning schemes are shown in Fig. 4 and reported in Table 2, together with the integrated measurements. For each scheme individually, the compatibility with the CP -symmetry hypothesis is evaluated by means of a χ^2 test, with $\chi^2 = R^T V^{-1} R$, where R is the array of $a_{CP}^{\tilde{T}\text{-odd}}$ measurements and V is the covariance matrix, which is the sum of the statistical and systematic covariance matrices. An average systematic uncertainty, whose evaluation is discussed below, is assigned for all bins. The systematic uncertainties are assumed to be fully correlated; their contribution is small compared to the statistical uncertainties. The p -values of the CP -symmetry hypothesis are 4.9×10^{-2} and 7.1×10^{-4} for schemes A and B, respectively, corresponding to statistical significances of 2.0 and 3.4 Gaussian standard deviations (σ). A similar χ^2 test is performed on $a_p^{\tilde{T}\text{-odd}}$ measurements with p -values for the P -symmetry hypothesis of 5.8×10^{-3} (2.8σ) and 2.4×10^{-2} (2.3σ), for scheme A and B, respectively. The overall significance for CPV in $\Lambda_b^0 \rightarrow p\pi^-\pi^+\pi^-$ decays from the results of schemes A and B is determined by means of a permutation test⁴⁴, taking into account correlations among the results. A sample of 40,000 pseudoexperiments is generated from the data by assigning each event a random $\Lambda_b^0/\bar{\Lambda}_b^0$ flavour such that CP symmetry is enforced. The sign of $C_{\tilde{T}}$ is unchanged if a Λ_b^0 candidate stays Λ_b^0 and reversed if the Λ_b^0 candidate becomes $\bar{\Lambda}_b^0$. The p -value of the CP -symmetry

hypothesis is determined as the fraction of pseudoexperiments with χ^2 larger than that measured in data. Applying this method to the χ^2 values from schemes A and B individually, the p -values obtained agree with those from the χ^2 test within the uncertainty due to the limited number of pseudoexperiments. To assess a combined significance from the two schemes, the product of the two p -values measured in data is compared with the distribution of the product of the p -values of the two binning schemes from the pseudoexperiments. The fraction of pseudoexperiments whose p -value product is smaller than that seen in data determines the overall p -value of the combination of the two schemes⁴⁵. An overall p -value of 9.8×10^{-4} (3.3σ) is obtained for the CP -symmetry hypothesis, including systematic uncertainties.

For the $\Lambda_b^0 \rightarrow p\pi^-K^+K^-$ decays, the smaller purity and signal yield of the sample do not permit PV and CPV to be probed with the same precision as for $\Lambda_b^0 \rightarrow p\pi^-\pi^+\pi^-$, and therefore only two regions of phase space are considered. One spans $1.43 < m(pK^-) < 2.00 \text{ GeV}/c^2$ (bin 1) and is dominated by excited Λ resonances decaying to pK and the other covers the remaining phase space, $2.00 < m(pK^-) < 4.99 \text{ GeV}/c^2$ (bin 2). The observables measured in these regions are given in Table 2 and are consistent with CP and P symmetry.

The main sources of systematic uncertainties for both $p\pi^-\pi^+\pi^-$ and $p\pi^-K^+K^-$ decays are experimental effects that could introduce biases in the measured asymmetries. This is tested by measuring the asymmetry $a_{CP}^{\tilde{T}\text{-odd}}$, integrated over phase space and in various phase space regions, using the control sample $\Lambda_b^0 \rightarrow \Lambda_c^+(pK^-\pi^+)\pi^-$, which is expected to exhibit negligible CPV. The results are in agreement with the CP -symmetry hypothesis; an uncertainty of 0.31% is assigned as a systematic uncertainty for the $a_{CP}^{\tilde{T}\text{-odd}}$ and $a_p^{\tilde{T}\text{-odd}}$ integrated measurements; an uncertainty of 0.60%, the largest asymmetry from a fit to scheme B measurements using a range of efficiency and fit models, is assigned for the corresponding phase space measurements. The systematic uncertainty arising from the experimental resolution in the measurement of the triple products $C_{\tilde{T}}$ and $\bar{C}_{\tilde{T}}$, which could introduce a migration of events between the bins, is estimated from simulated samples of $\Lambda_b^0 \rightarrow p\pi^-\pi^+\pi^-$ and $\Lambda_b^0 \rightarrow p\pi^-K^+K^-$ decays where neither P - nor CP -violating effects are present. The difference between the reconstructed and generated asymmetry is taken as a systematic uncertainty due to this effect, and is less than 0.06% in all cases. To assess the uncertainty associated

Table 2 | Measurements of CP- and P-violating observables.

	$a_{\hat{P}}^{\hat{T}\text{-odd}} [\%]$	$a_{\hat{CP}}^{\hat{T}\text{-odd}} [\%]$
Scheme A		
	$\Lambda_b^0 \rightarrow p\pi^- \pi^+ \pi^-$	
1	$21.64 \pm 8.28 \pm 0.60$	$-7.69 \pm 8.28 \pm 0.60$
2	$-2.04 \pm 3.26 \pm 0.60$	$-0.33 \pm 3.26 \pm 0.60$
3	$2.03 \pm 6.12 \pm 0.60$	$1.94 \pm 6.12 \pm 0.60$
4	$-2.45 \pm 4.60 \pm 0.60$	$-3.49 \pm 4.60 \pm 0.60$
5	$-10.04 \pm 4.13 \pm 0.60$	$10.29 \pm 4.13 \pm 0.60$
6	$-6.40 \pm 5.23 \pm 0.60$	$6.51 \pm 5.23 \pm 0.60$
7	$-11.91 \pm 5.00 \pm 0.60$	$8.40 \pm 5.00 \pm 0.60$
8	$0.94 \pm 5.60 \pm 0.60$	$-1.88 \pm 5.60 \pm 0.60$
9	$-5.38 \pm 4.67 \pm 0.60$	$7.20 \pm 4.67 \pm 0.60$
10	$-4.26 \pm 4.98 \pm 0.60$	$-11.24 \pm 4.98 \pm 0.60$
11	$13.94 \pm 7.19 \pm 0.60$	$-2.90 \pm 7.19 \pm 0.60$
12	$-7.64 \pm 4.79 \pm 0.60$	$-5.35 \pm 4.79 \pm 0.60$
Scheme B		
1	$-0.42 \pm 4.92 \pm 0.60$	$1.81 \pm 4.92 \pm 0.60$
2	$-1.63 \pm 4.88 \pm 0.60$	$2.86 \pm 4.88 \pm 0.60$
3	$-14.73 \pm 5.13 \pm 0.60$	$2.87 \pm 5.13 \pm 0.60$
4	$-0.32 \pm 4.95 \pm 0.60$	$19.79 \pm 4.95 \pm 0.60$
5	$-2.71 \pm 5.16 \pm 0.60$	$4.47 \pm 5.16 \pm 0.60$
6	$-3.85 \pm 4.79 \pm 0.60$	$-7.23 \pm 4.79 \pm 0.60$
7	$-14.40 \pm 4.65 \pm 0.60$	$-5.44 \pm 4.65 \pm 0.60$
8	$-3.75 \pm 4.14 \pm 0.60$	$0.76 \pm 4.14 \pm 0.60$
9	$-4.16 \pm 4.01 \pm 0.60$	$7.74 \pm 4.01 \pm 0.60$
10	$4.21 \pm 3.84 \pm 0.60$	$-9.16 \pm 3.84 \pm 0.60$
Integrated	$-3.71 \pm 1.45 \pm 0.32$	$1.15 \pm 1.45 \pm 0.32$
Phase space bin		
	$\Lambda_b^0 \rightarrow p\pi^- K^+ K^-$	
1	$3.27 \pm 6.07 \pm 0.66$	$-4.68 \pm 6.07 \pm 0.66$
2	$4.43 \pm 6.73 \pm 0.66$	$4.73 \pm 6.73 \pm 0.66$
Integrated	$3.62 \pm 4.54 \pm 0.42$	$-0.93 \pm 4.54 \pm 0.42$

The CP- and P-violating observables, $a_{\hat{P}}^{\hat{T}\text{-odd}}$ and $a_{\hat{CP}}^{\hat{T}\text{-odd}}$, resulting from the fit to the data are listed with their statistical and systematic uncertainties. Each value is obtained through an independent fit to a region of the phase space as described in the text and Table 1. Results for schemes A and B are outlined for $\Lambda_b^0 \rightarrow p\pi^- \pi^+ \pi^-$ decays, and in two bins of phase space for $\Lambda_b^0 \rightarrow p\pi^- K^+ K^-$ decays, as defined in the text. The first column lists the bin number. For both decay modes the measurement integrated over the phase space, performed independently, is also shown.

with the fit models, alternative functions are used; these tests lead only to small changes in the asymmetries, the largest being 0.05%. For $\Lambda_b^0 \rightarrow p\pi^- K^+ K^-$ decays, this contribution is larger, about 0.28% for the $a_{\hat{CP}}^{\hat{T}\text{-odd}}$ and $a_{\hat{P}}^{\hat{T}\text{-odd}}$ asymmetries.

Further cross-checks are made to investigate the stability of the results with respect to different periods of recording data, different polarities of the spectrometer magnet, the choice made in the selection of multiple candidates, and the effect of the trigger and selection criteria. Alternative binning schemes are studied as a cross-check, such as using 8 or 12 bins in $|\Phi|$ for $\Lambda_b^0 \rightarrow p\pi^- \pi^+ \pi^-$ decays. For these alternative binning schemes, the significance of the CPV measurement of the modified scheme B is reduced to below 3σ . Nonetheless, the overall significance of the combination of these two additional binnings with schemes A and B remains above three standard deviations, with a p -value of 1.8×10^{-3} (3.1σ), consistent with the 3.3σ result seen in the baseline analysis. An independent analysis of the data based on alternative selection criteria confirmed the results. It used a similar number of events, of which 73.4% are in common with the baseline analysis, and gave p -values for CP symmetry of 3.4×10^{-3} (2.9σ) for scheme A and 1.4×10^{-4} (3.8σ) for scheme B.

In conclusion, a search for P and CP violation in $\Lambda_b^0 \rightarrow p\pi^- \pi^+ \pi^-$ and $\Lambda_b^0 \rightarrow p\pi^- K^+ K^-$ decays is performed on signal yields of $6,646 \pm 105$ and $1,030 \pm 56$ events. This is

the first observation of these decay modes. Measurements of asymmetries in the entire phase space do not show any evidence of P or CP violation. Searches for localized P or CP violation are performed by measuring asymmetries in different regions of the phase space. The results are consistent with CP symmetry for $\Lambda_b^0 \rightarrow p\pi^- K^+ K^-$ decays, but evidence for CP violation at the 3.3σ level is found in $\Lambda_b^0 \rightarrow p\pi^- \pi^+ \pi^-$ decays. No significant P violation is found. This represents the first evidence of CP violation in the baryon sector, and indicates an asymmetry between baryonic matter and antimatter.

Data availability. All data shown in histograms and plots are publicly available from HEPdata (<https://hepdata.net>).

Received 16 September 2016; accepted 21 December 2016; published online 30 January 2017

References

- Cabibbo, N. Unitary symmetry and leptonic decays. *Phys. Rev. Lett.* **10**, 531–533 (1963).
- Kobayashi, M. & Maskawa, T. CP violation in the renormalizable theory of weak interaction. *Prog. Theor. Phys.* **49**, 652–657 (1973).
- Sakharov, A. D. Violation of CP invariance, C asymmetry, and baryon asymmetry of the universe. *JETP Lett.* **5**, 24–27 (1967); *Sov. Phys. Usp.* **34**, 392–393 (1991).
- Riotto, A. Theories of Baryogenesis. in *In Proc. Summer School in High-energy Physics and Cosmology* (eds Gava, E. et al.) 326–436 (World Scientific, 1998).
- Christenson, J. H., Cronin, J. W., Fitch, V. L. & Turlay, R. Evidence for the 2π decay of the K_S^0 Meson. *Phys. Rev. Lett.* **13**, 138–140 (1964).
- Aubert, B. et al. Observation of CP violation in the B^0 meson system. *Phys. Rev. Lett.* **87**, 091801 (2001).
- Abe, K. et al. Observation of large CP violation in the neutral B meson system. *Phys. Rev. Lett.* **87**, 091802 (2001).
- Aubert, B. et al. Improved measurement of the CKM angle γ in $B^\pm \rightarrow D^{(*)} K^{(*)\mp}$ decays with a Dalitz plot analysis of D decays to $K_S^0 \pi^+ \pi^-$ and $K_S^0 K^+ K^-$. *Phys. Rev. D* **78**, 034023 (2008).
- Poluektov, A. et al. Evidence for direct CP violation in the decay $B^+ \rightarrow D^{(*)} K^+$, $D \rightarrow K^+ \pi^+ \pi^-$ and measurement of the CKM phase ϕ_3 . *Phys. Rev. D* **81**, 112002 (2010).
- Aaij, R. et al. Observation of CP violation in $B^\pm \rightarrow DK^\pm$ decays. *Phys. Lett. B* **712**, 203–212 (2012); erratum **713**, 351 (2012).
- Aaij, R. et al. Measurement of CP violation in the phase space of $B^\pm \rightarrow K^\pm \pi^+ \pi^-$ and $B^\pm \rightarrow K^\pm K^+ K^-$ decays. *Phys. Rev. Lett.* **111**, 101801 (2013).
- Aaij, R. et al. First observation of CP violation in the decays of B_s^0 mesons. *Phys. Rev. Lett.* **110**, 221601 (2013).
- Hsiao, Y. K. & Geng, C. Q. Direct CP violation in Λ_b^0 decays. *Phys. Rev. D* **91**, 116007 (2015).
- Bensalem, W. & London, D. T-odd triple-product correlations in hadronic b decays. *Phys. Rev. D* **64**, 116003 (2001).
- Bensalem, W., Datta, A. & London, D. New physics effects on triple-product correlations in Λ_b^0 decays. *Phys. Rev. D* **66**, 094004 (2002).
- Bensalem, W., Datta, A. & London, D. T-violating triple-product correlations in charmless Λ_b^0 decays. *Phys. Lett. B* **538**, 309–320 (2002).
- Sachs, R. G. *The Physics of Time Reversal* (Univ. Chicago Press, 1987).
- Branco, G. C., Lavoura, L. & Silva, J. P. *CP Violation* (Oxford Univ. Press, 1999).
- Durieux, G. & Grossman, Y. Probing CP violation systematically in differential distributions. *Phys. Rev. D* **92**, 076013 (2015).
- Durieux, G. CP violation in multibody decays of beauty baryons. *JHEP* **10**, 005 (2016).
- Gasiorowicz, S. *Elementary particle physics* (Wiley, 1966).
- Bigi, I. I. Y. Charm Physics: Like Botticelli in the Sistine Chapel. Preprint at <https://arxiv.org/abs/hep-ph/0107102> (2001).
- Gronau, M. & Rosner, J. L. Triple product asymmetries in K , $D_{(s)}$ and $B_{(s)}$ decays. *Phys. Rev. D* **84**, 096013 (2011).
- Gronau, M. & Rosner, J. L. Triple product asymmetries in Λ_b^0 and Ξ_b^0 decays. *Phys. Lett. B* **749**, 104–107 (2015).
- Valencia, G. Angular correlations in the decay $B \rightarrow VV$ and CP violation. *Phys. Rev. D* **39**, 3339–3345 (1989).
- Aaij, R. et al. Search for CP violation using T-odd correlations in $D^0 \rightarrow K^+ K^- \pi^+ \pi^-$ decays. *JHEP* **10**, 005 (2014).
- Aaij, R. et al. Measurement of b-hadron production fractions in 7 TeV pp collisions. *Phys. Rev. D* **85**, 032008 (2012).

28. Aaij, R. *et al.* Study of the kinematic dependences of Λ_b^0 production in pp collisions and a measurement of the $\Lambda_b^0 \rightarrow \Lambda_c^+ \pi^-$ branching fraction. *JHEP* **08**, 143 (2014).
29. Alves, A. A. Jr *et al.* The LHCb detector at the LHC. *JINST* **3**, S08005 (2008).
30. Aaij, R. *et al.* LHCb detector performance. *Int. J. Mod. Phys. A* **30**, 1530022 (2015).
31. LHCb collaboration. *LHC-B: A Dedicated LHC Collider Beauty Experiment for Precision Measurements of CP Violation* Letter of intent (CERN-LHCC-95-05, 1995); <http://cds.cern.ch/record/290868>
32. Sjöstrand, T., Mrenna, S. & Skands, P. PYTHIA 6.4 physics and manual. *JHEP* **05**, 026 (2006).
33. Sjöstrand, T., Mrenna, S. & Skands, P. A brief introduction to PYTHIA 8.1. *Comput. Phys. Commun.* **178**, 852–867 (2008).
34. Belyaev, I. *et al.* Handling of the generation of primary events in Gauss, the LHCb simulation framework. *J. Phys. Conf. Ser.* **331**, 032047 (2011).
35. Lange, D. J. The EvtGen particle decay simulation package. *Nucl. Instrum. Meth. A* **462**, 152–155 (2001).
36. Allison, J. *et al.* Geant4 developments and applications. *IEEE Trans. Nucl. Sci.* **53**, 270–278 (2006).
37. Agostinelli, S. *et al.* Geant4: A simulation toolkit. *Nucl. Instrum. Meth. A* **506**, 250–303 (2003).
38. Clemencic, M. *et al.* The LHCb simulation application, Gauss: design, evolution and experience. *J. Phys. Conf. Ser.* **331**, 032023 (2011).
39. Olive, K. A. *et al.* Review of particle physics. *Chin. Phys. C* **38**, 090001 (2014).
40. Breiman, L., Friedman, J. H., Olshen, R. A. & Stone, C. J. *Classification and Regression Trees* (Wadsworth International Group, 1984).
41. Pivk, M. & Le Diberder, F. R. sPlot: a statistical tool to unfold data distributions. *Nucl. Instrum. Meth. A* **555**, 356–369 (2005).
42. Skwarnicki, T. *A study of the radiative CASCADE transitions between the Upsilon-Prime and Upsilon resonances* (Ph.D. thesis, 1986); <https://inspirehep.net/record/230779>
43. Albrecht, H. *et al.* Search for hadronic $b \rightarrow u$ decays. *Phys. Lett. B* **241**, 278–282 (1990).
44. Fisher, R. A. *The design of experiments* (Oliver and Boyd Ltd., 1935).
45. *Data analysis in high energy physics* (eds Behnke, O., Kröninger, K., Schörner-Sadenius, T. & Schott, G.) (Wiley, 2013).

Acknowledgements

We express our gratitude to our colleagues in the CERN accelerator departments for the excellent performance of the LHC. We thank the technical and administrative staff at the

LHCb institutes. We acknowledge support from CERN and from the national agencies: CAPES, CNPq, FAPERJ and FINEP (Brazil); NSFC (China); CNRS/IN2P3 (France); BMBF, DFG and MPG (Germany); INFN (Italy); FOM and NWO (The Netherlands); MNiSW and NCN (Poland); MEN/IFA (Romania); MinES and FASO (Russia); MinECO (Spain); SNSF and SER (Switzerland); NASU (Ukraine); STFC (United Kingdom); NSF (USA). We acknowledge the computing resources that are provided by CERN, IN2P3 (France), KIT and DESY (Germany), INFN (Italy), SURF (The Netherlands), PIC (Spain), GridPP (United Kingdom), RRCKI and Yandex LLC (Russia), CSCS (Switzerland), IFIN-HH (Romania), CBPF (Brazil), PL-GRID (Poland) and OSC (USA). We are indebted to the communities behind the multiple open source software packages on which we depend. Individual groups or members have received support from AvH Foundation (Germany), EPLANET, Marie Skłodowska-Curie Actions and ERC (European Union), Conseil Général de Haute-Savoie, Labex ENIGMASS and OCEVU, Région Auvergne (France), RFBR and Yandex LLC (Russia), GVA, XuntaGal and GENCAT (Spain), Herchel Smith Fund, The Royal Society, Royal Commission for the Exhibition of 1851 and the Leverhulme Trust (United Kingdom).

Author contributions

All authors have contributed to the publication, being variously involved in the design and the construction of the detectors, in writing software, calibrating sub-systems, operating the detectors and acquiring data, and finally analysing the processed data.

Additional information

Reprints and permissions information is available online at www.nature.com/reprints. Correspondence and requests for materials should be addressed to N. Neri (nicola.neri@mi.infn.it).

Competing financial interests

The authors declare no competing financial interests.



This article is licensed under a Creative Commons Attribution 4.0 International License, which permits use, sharing, adaptation, distribution and reproduction in any medium or format, as long as you give appropriate credit to the original author(s) and the source, provide a link to the Creative Commons license, and indicate if changes were made.

The images or other third party material in this article are included in the article's Creative Commons license, unless indicated otherwise in a credit line to the material. If material is not included in the article's Creative Commons license and your intended use is not permitted by statutory regulation or exceeds the permitted use, you will need to obtain permission directly from the copyright holder. To view a copy of this license, visit <http://creativecommons.org/licenses/by/4.0/>.

The LHCb collaboration

R. Aaij⁴⁰, B. Adeva³⁹, M. Adinolfi⁴⁸, Z. Ajaltouni⁵, S. Akar⁶, J. Albrecht¹⁰, F. Alessio⁴⁰, M. Alexander⁵³, S. Ali⁴³, G. Alkhazov³¹, P. Alvarez Cartelle⁵⁵, A. A. Alves Jr.⁵⁹, S. Amato², S. Amerio²³, Y. Amhis⁷, L. An⁴¹, L. Anderlini¹⁸, G. Andreassi⁴¹, M. Andreotti^{17,g}, J. E. Andrews⁶⁰, R. B. Appleby⁵⁶, F. Archilli⁴³, P. d'Argent¹², J. Arnau Romeu⁶, A. Artamonov³⁷, M. Artuso⁶¹, E. Aslanides⁶, G. Auremma²⁶, M. Baalouch⁵, I. Babuschkin⁵⁶, S. Bachmann¹², J. J. Back⁵⁰, A. Badalov³⁸, C. Baesso⁶², S. Baker⁵⁵, W. Baldini¹⁷, R. J. Barlow⁵⁶, C. Barschel⁴⁰, S. Barsuk⁷, W. Barter⁴⁰, M. Baszczyk²⁷, V. Batozskaya²⁹, B. Batsukh⁶¹, V. Battista⁴¹, A. Bay⁴¹, L. Beaucourt⁴, J. Beddow⁵³, F. Bedeschi²⁴, I. Bediaga¹, L. J. Bel⁴³, V. Bellee⁴¹, N. Belloli^{21,i}, K. Belous³⁷, I. Belyaev³², E. Ben-Haim⁸, G. Bencivenni¹⁹, S. Benson⁴³, J. Benton⁴⁸, A. Berezhnoy³³, R. Bernet⁴², A. Bertolin²³, F. Betti¹⁵, M.-O. Bettler⁴⁰, M. van Beuzekom⁴³, I. Bezshyiko⁴², S. Bifani⁴⁷, P. Billoir⁸, T. Bird⁵⁶, A. Birnkraut¹⁰, A. Bitadze⁵⁶, A. Bizzeti^{18,u}, T. Blake⁵⁰, F. Blanc⁴¹, J. Blouin¹¹, S. Blusk⁶¹, V. Bocci²⁶, T. Boettcher⁵⁸, A. Bondar³⁶, N. Bondar^{31,40}, W. Bonivento¹⁶, A. Borgheresi^{21,i}, S. Borghi⁵⁶, M. Borisyak³⁵, M. Borsato³⁹, F. Bossu⁷, M. Boubdir⁹, T. J. V. Bowcock⁵⁴, E. Bowen⁴², C. Bozzi^{17,40}, S. Braun¹², M. Britsch¹², T. Britton⁶¹, J. Brodzicka⁵⁶, E. Buchanan⁴⁸, C. Burr⁵⁶, A. Bursche², J. Buytaert⁴⁰, S. Cadeddu¹⁶, R. Calabrese^{17,g}, M. Calvi^{21,i}, M. Calvo Gomez^{38,m}, A. Camboni³⁸, P. Campana¹⁹, D. Campora Perez⁴⁰, D. H. Campora Perez⁴⁰, L. Capriotti⁵⁶, A. Carbone^{15,e}, G. Carboni^{25,j}, R. Cardinale^{20,h}, A. Cardini¹⁶, P. Carniti^{21,i}, L. Carson⁵², K. Carvalho Akiba², G. Casse⁵⁴, L. Cassina^{21,i}, L. Castillo Garcia⁴¹, M. Cattaneo⁴⁰, Ch. Cauet¹⁰, G. Cavallero²⁰, R. Cenci^{24,t}, M. Charles⁸, Ph. Charpentier⁴⁰, G. Chatzikonstantinidis⁴⁷, M. Chefdeville⁴, S. Chen⁵⁶, S.-F. Cheung⁵⁷, V. Chobanova³⁹, M. Chrzasczcz^{42,27}, X. Cid Vidal³⁹, G. Ciezarek⁴³, P. E. L. Clarke⁵², M. Clemencic⁴⁰, H. V. Cliff⁴⁹, J. Closier⁴⁰, V. Coco⁵⁹, J. Cogan⁶, E. Cogneras⁵, V. Cogoni^{16,40,f}, L. Cojocariu³⁰, G. Collazuol^{23,o}, P. Collins⁴⁰, A. Comerma-Montells¹², A. Contu⁴⁰, A. Cook⁴⁸, S. Coquereau³⁸, G. Corti⁴⁰, M. Corvo^{17,g}, C. M. Costa Sobral⁵⁰, B. Couturier⁴⁰, G. A. Cowan⁵², D. C. Craik⁵², A. Crocombe⁵⁰, M. Cruz Torres⁶², S. Cunliffe⁵⁵, R. Currie⁵⁵, C. D'Ambrosio⁴⁰, F. Da Cunha Marinho², E. Dall'Occo⁴³, J. Dalseno⁴⁸, P. N. Y. David⁴³, A. Davis⁵⁹, O. De Aguiar Francisco², K. De Bruyn⁶, S. De Capua⁵⁶, M. De Cian¹², J. M. De Miranda¹, L. De Paula², M. De Serio^{14,d}, P. De Simone¹⁹, C.-T. Dean⁵³, D. Decamp⁴, M. Deckenhoff¹⁰, L. Del Buono⁸, M. Demmer¹⁰, D. Derkach³⁵, O. Deschamps⁵, F. Dettori⁴⁰, B. Dey²², A. Di Canto⁴⁰, H. Dijkstra⁴⁰, F. Dordei⁴⁰, M. Dorigo⁴¹, A. Dosil Suárez³⁹, A. Dovbnya⁴⁵, K. Dreimanis⁵⁴, L. Dufour⁴³, G. Dujany⁵⁶, K. Dungs⁴⁰, P. Durante⁴⁰, R. Dzhylyadin⁵², A. Dziurda⁴⁰, A. Dzyuba³¹, N. Déleage⁴, S. Easo⁵¹, M. Ebert⁵², U. Egede⁵⁵, V. Egorychev³², S. Eidelman³⁶, S. Eisenhardt⁵², U. Eitschberger¹⁰, R. Ekelhof¹⁰, L. Eklund⁵³, Ch. Elsasser⁴², S. Ely⁶¹, S. Esen¹², H. M. Evans⁴⁹, T. Evans⁵⁷, A. Falabella¹⁵, N. Farley⁴⁷, S. Farry⁵⁴, R. Fay⁵⁴, D. Fazzini^{21,i}, D. Ferguson⁵², V. Fernandez Albor³⁹, A. Fernandez Prieto³⁹, F. Ferrari^{15,40}, F. Ferreira Rodrigues¹, M. Ferro-Luzzi⁴⁰, S. Filippov³⁴, R. A. Fini¹⁴, M. Fiore^{17,g}, M. Fiorini^{17,g}, M. Firlje²⁸, C. Fitzpatrick⁴¹, T. Fiutowski²⁸, F. Fleuret^{7,b}, K. Fohl⁴⁰, M. Fontana^{16,40}, F. Fontanelli^{20,h}, D. C. Forshaw⁶¹, R. Forty⁴⁰, V. Franco Lima⁵⁴, M. Frank⁴⁰, C. Frei⁴⁰, J. Fu^{22,q}, E. Furfaro^{25,j}, C. Färber⁴⁰, A. Gallas Torreira³⁹, D. Galli^{15,e}, S. Gallorini²³, S. Gambetta⁵², M. Gandelman², P. Gandini⁵⁷, Y. Gao³, L. M. Garcia Martin⁶², J. Garcia Pardiñas³⁹, J. Garra Tico⁴⁹, L. Garrido³⁸, P. J. Garsed⁴⁹, D. Gascon³⁸, C. Gaspar⁴⁰, L. Gavardi¹⁰, G. Gazzoni⁵, D. Gerick¹², E. Gersabeck¹², M. Gersabeck⁵⁶, T. Gershon⁵⁰, Ph. Ghez⁴, S. Giani⁴¹, V. Gibson⁴⁹, O. G. Girard⁴¹, L. Giubega³⁰, K. Gizdov⁵², V. V. Gligorov⁸, D. Golubkov³², A. Golutvin^{55,40}, A. Gomes^{1,a}, I. V. Gorelov³³, C. Gotti^{21,i}, M. Grabalosa Gándara⁵, R. Graciani Diaz³⁸, L. A. Granado Cardoso⁴⁰, E. Graugés³⁸, E. Graverini⁴², G. Graziani¹⁸, A. Grecu³⁰, P. Griffith⁴⁷, L. Grillo^{21,40,i}, B. R. Gruberg Cazon⁵⁷, O. Grünberg⁶⁶, E. Gushchin³⁴, Yu. Guz³⁷, T. Gys⁴⁰, C. Göbel⁶², T. Hadavizadeh⁵⁷, C. Hadjivasiliou⁵, G. Haefeli⁴¹, C. Haen⁴⁰, S. C. Haines⁴⁹, S. Hall⁵⁵, B. Hamilton⁶⁰, X. Han¹², S. Hansmann-Menzemer¹², N. Harnew⁵⁷, S. T. Harnew⁴⁸, J. Harrison⁵⁶, M. Hatch⁴⁰, J. He⁶³, T. Head⁴¹, A. Heister⁹, K. Hennessy⁵⁴, P. Henrard⁵⁴, L. Henry⁸, J. A. Hernandez Morata³⁹, E. van Herwijnen⁴⁰, M. Heß⁶⁶, A. Hicheur², D. Hill⁵⁷, C. Hombach⁵⁶, H. Hopchev⁴¹, W. Hulsbergen⁴³, T. Humair⁵⁵, M. Hushchyn³⁵, N. Hussain⁵⁷, D. Hutchcroft⁵⁴, M. Idzik²⁸, P. Ilten⁵⁸, R. Jacobsson⁴⁰, A. Jaeger¹², J. Jaloča⁵⁷, E. Jans⁴³, A. Jawahery⁶⁰, F. Jiang³, M. John⁵⁷, D. Johnson⁴⁰, C. R. Jones⁴⁹, C. Joram⁴⁰, B. Jost⁴⁰, N. Jurik⁶¹, S. Kandybei⁴⁵, W. Kanso⁶, M. Karacson⁴⁰, J. M. Kariuki⁴⁸, S. Karodia⁵³, M. Kecke¹², M. Kelsey⁶¹, I. R. Kenyon⁴⁷, M. Kenzie⁴⁹, T. Ketel¹⁴, E. Khairullin³⁵, B. Khanji^{21,40,i}, C. Khurewathanakul⁴¹, T. Kirn⁹, S. Klaver⁵⁶, K. Klimaszewski²⁹, S. Koliiev⁴⁶, M. Kolpin¹², I. Komarov⁴¹, R. F. Koopman⁴⁴, P. Koppenburg⁴³, A. Kozachuk³³, M. Kozeiha⁵, L. Kravchuk³⁴, K. Kreplin¹², M. Kreps⁵⁰, P. Krokovny³⁶, F. Kruse¹⁰, W. Krzemien²⁹, W. Kucewicz^{27,1}, M. Kucharczyk²⁷, V. Kudryavtsev³⁶, A. K. Kuonen⁴¹, K. Kurek²⁹, T. Kvaratskheliya^{32,40}, D. Lacarrere⁴⁰, G. Lafferty⁵⁶, A. Lai¹⁶, D. Lambert⁵², G. Lanfranchi¹⁹, C. Langenbruch⁹, T. Latham⁵⁰, C. Lazzeroni⁴⁷, R. Le Gac⁶, J. van Leerdam⁴³, J.-P. Lees⁴, A. Leflat^{33,40}, J. Lefrançois⁷, R. Lefèvre⁵, F. Lemaître⁴⁰, E. Lemos Cid³⁹, O. Lery⁶, T. Lesiak²⁷, B. Leverington¹², Y. Li⁷, T. Likhomanenko^{35,67}, R. Lindner⁴⁰, C. Linn⁴⁰, F. Lionetto⁴², B. Liu¹⁶, X. Liu³, D. Loh⁵⁰, I. Longstaff⁵³, J. H. Lopes², D. Lucchesi^{23,o}, M. Lucio Martinez³⁹, H. Luo⁵², A. Lupato²³, E. Luppi^{17,g}, O. Lupton⁵⁷, A. Lusiani²⁴, X. Lyu⁶³, F. Machefert⁷, F. Maciuc³⁰, O. Maev³¹, K. Maguire⁵⁶, S. Malde⁵⁷, A. Malinin⁶⁷, T. Maltsev³⁶, G. Manca⁷, G. Mancinelli⁶, P. Manning⁶¹, J. Maratas^{5,v}, J. F. Marchand⁴, U. Marconi¹⁵, C. Marin Benito³⁸, P. Marino^{24,t}, J. Marks¹², G. Martellotti²⁶, M. Martin⁶, M. Martinelli⁴¹, D. Martinez Santos³⁹, F. Martinez Vidal⁶⁸, D. Martins Tostes², L. M. Massacrier⁷, A. Massafferri¹, R. Matev⁴⁰, A. Mathad⁵⁰, Z. Mathe⁴⁰, C. Matteuzzi²¹, A. Mauri⁴², B. Maurin⁴¹, A. Mazurov⁴⁷, M. McCann⁵⁵, J. McCarthy⁴⁷, A. McNab⁵⁶, R. McNulty¹³, B. Meadows⁵⁹, F. Meier¹⁰, M. Meissner¹², D. Melnychuk²⁹, M. Merk⁴³, A. Merli^{22,q}, E. Michielin²³, D. A. Milanes⁶⁵, M.-N. Minard⁴, D. S. Mitzel¹², A. Mogini⁸, J. Molina Rodriguez⁶², I. A. Monroy⁶⁵, S. Monteil⁵, M. Morandin²³, P. Morawski²⁸, A. Mordà⁶, M. J. Morello^{24,t}, J. Moron²⁸, A. B. Morris⁵², R. Mountain⁶¹, F. Muheim⁵², M. Mulder⁴³, M. Mussini¹⁵, D. Müller⁵⁶, J. Müller¹⁰, K. Müller⁴², V. Müller¹⁰, P. Naik⁴⁸, T. Nakada⁴¹, R. Nandakumar⁵¹, A. Nandi⁵⁷, I. Nasteva², M. Needham⁵², N. Neri²², S. Neubert¹², N. Neufeld⁴⁰, M. Neuner¹², A. D. Nguyen⁴¹, C. Nguyen-Mau^{41,n}

S. Nieswand⁹, R. Niet¹⁰, N. Nikitin³³, T. Nikodem¹², A. Novoselov³⁷, D. P. O'Hanlon⁵⁰, A. Oblakowska-Mucha²⁸, V. Obraztsov³⁷, S. Ogilvy¹⁹, R. Oldeman⁴⁹, C. J. G. Onderwater⁶⁹, J. M. Otorola Goicochea², A. Otto⁴⁰, P. Owen⁴², A. Oyanguren⁶⁸, P. R. Pais⁴¹, A. Palano^{14,d}, F. Palombo^{22,q}, M. Palutan¹⁹, J. Panman⁴⁰, A. Papanestis⁵¹, M. Pappagallo^{14,d}, L. L. Pappalardo^{17,g}, W. Parker⁶⁰, C. Parkes⁵⁶, G. Passaleva¹⁸, A. Pastore^{14,d}, G. D. Patel⁵⁴, M. Patel⁵⁵, C. Patrignani^{15,e}, A. Pearce^{56,51}, A. Pellegrino⁴³, G. Penso²⁶, M. Pepe Altarelli⁴⁰, S. Perazzini⁴⁰, P. Perret⁵, L. Pescatore⁴⁷, K. Petridis⁴⁸, A. Petrolini^{20,h}, A. Petrov⁶⁷, M. Petruzzo^{22,q}, E. Picatoste Olloqui³⁸, B. Pietrzyk⁴, M. Piekies²⁷, D. Pinci²⁶, A. Pistone²⁰, A. Piucci¹², S. Playfer⁵², M. Plo Casasus³⁹, T. Poikela⁴⁰, F. Polci⁸, A. Poluektov^{50,36}, I. Polyakov⁶¹, E. Polcarpo², G. J. Pomery⁴⁸, A. Popov³⁷, D. Popov^{11,40}, B. Popovici³⁰, S. Poslavskii³⁷, C. Potterat², E. Price⁴⁸, J. D. Price⁵⁴, J. Prisciandaro³⁹, A. Pritchard⁵⁴, C. Prouve⁴⁸, V. Pugatch⁴⁶, A. Puig Navarro⁴¹, G. Punzi^{24,p}, W. Qian⁵⁷, R. Quagliani^{7,48}, B. Rachwal²⁷, J. H. Rademacker⁴⁸, M. Rama²⁴, M. Ramos Pernas³⁹, M. S. Rangel², I. Raniuk⁴⁵, G. Raven⁴⁴, F. Redi⁵⁵, S. Reichert¹⁰, A. C. dos Reis¹, C. Remon Alepuz⁶⁸, V. Renaudin⁷, S. Ricciardi⁵¹, S. Richards⁴⁸, M. Rihl⁴⁰, K. Rinnert⁵⁴, V. Rives Molina³⁸, P. Robbe^{7,40}, A. B. Rodrigues¹, E. Rodrigues⁵⁹, J. A. Rodriguez Lopez⁶⁵, P. Rodriguez Perez⁵⁶, A. Rogozhnikov³⁵, S. Roiser⁴⁰, V. Romanovskiy³⁷, A. Romero Vidal³⁹, J. W. Ronayne¹³, M. Rotondo¹⁹, M. S. Rudolph⁶¹, T. Ruf⁴⁰, P. Ruiz Valls⁶⁸, J. J. Saborido Silva³⁹, E. Sadykhov³², N. Sagidova³¹, B. Saitta^{16,f}, V. Salustino Guimaraes², C. Sanchez Mayordomo⁶⁸, B. Sanmartin Sedes³⁹, R. Santacesaria²⁶, C. Santamarina Rios³⁹, M. Santimaria¹⁹, E. Santovetti^{25,j}, A. Sarti^{19,k}, C. Satriano^{26,s}, A. Satta²⁵, D. M. Saunders⁴⁸, D. Savrina^{32,33}, S. Schael⁹, M. Schellenberg¹⁰, M. Schiller⁴⁰, H. Schindler⁴⁰, M. Schlupp¹⁰, M. Schmelling¹¹, T. Schmelzer¹⁰, B. Schmidt⁴⁰, O. Schneider⁴¹, A. Schopper⁴⁰, K. Schubert¹⁰, M. Schubiger⁴¹, M.-H. Schune⁷, R. Schwemmer⁴⁰, B. Sciascia¹⁹, A. Sciubba^{26,k}, A. Semennikov³², A. Sergi⁴⁷, N. Serra⁴², J. Serrano⁶, L. Sestini²³, P. Seyfert²¹, M. Shapkin³⁷, I. Shapoval⁴⁵, Y. Shcheglov³¹, T. Shears⁵⁴, L. Shekhtman³⁶, V. Shevchenko⁶⁷, A. Shires¹⁰, B. G. Siddi^{17,40}, R. Silva Coutinho⁴², L. Silva de Oliveira², G. Simi^{23,o}, S. Simone^{14,d}, M. Sirendi⁴⁹, N. Skidmore⁴⁸, T. Skwarnicki⁶¹, E. Smith⁵⁵, I. T. Smith⁵², J. Smith⁴⁹, M. Smith⁵⁵, H. Snoek⁴³, M. D. Sokoloff⁵⁹, F. J. P. Soler⁵³, B. Souza De Paula², B. Spaan¹⁰, P. Spradlin⁵³, S. Sridharan⁴⁰, F. Stagni⁴⁰, M. Stahl¹², S. Stahl⁴⁰, P. Stefko⁴¹, S. Stefkova⁵⁵, O. Steinkamp⁴², S. Stemmler¹², O. Stenyakin³⁷, S. Stevenson⁵⁷, S. Stoica³⁰, S. Stone⁶¹, B. Storaci⁴², S. Stracka^{24,p}, M. Straticiu³⁰, U. Straumann⁴², L. Sun⁵⁹, W. Sutcliffe⁵⁵, K. Swientek²⁸, V. Syropoulos⁴⁴, M. Szczekowski²⁹, T. Szumlak²⁸, S. T'Jampens⁴, A. Taidyuganov⁶, T. Tekaampe¹⁰, G. Tellarini^{17,g}, F. Teubert⁴⁰, E. Thomas⁴⁰, J. van Tilburg⁴³, M. J. Tilley⁵⁵, V. Tisserand⁴, M. Tobin⁴¹, S. Tol⁴⁹, L. Tomassetti^{17,g}, D. Tonelli⁴⁰, S. Topp-Joergensen⁵⁷, F. Toriello⁶¹, E. Tournefier⁴, S. Tourneur⁴¹, K. Trabelsi⁴¹, M. Traill⁵³, M. T. Tran⁴¹, M. Tresch⁴², A. Trisovic⁴⁰, A. Tsaregorodtsev⁶, P. Tsopelas⁴³, A. Tully⁴⁹, N. Tuning⁴³, A. Ukleja²⁹, A. Ustyuzhanin^{35,67}, U. Uwer¹², C. Vacca^{16,f}, V. Vagnoni^{15,40}, A. Valassi⁴⁰, S. Valat⁴⁰, G. Valenti¹⁵, A. Vallier⁷, R. Vazquez Gomez¹⁹, P. Vazquez Regueiro³⁹, S. Vecchi¹⁷, M. van Veghel⁴³, J. J. Velthuis⁴⁸, M. Veltri^{18,r}, G. Veneziano⁴¹, A. Venkateswaran⁶¹, M. Vernet⁵, M. Vesterinen¹², B. Viaud⁷, D. Vieira¹, M. Vieites Diaz³⁹, X. Vilasis-Cardona^{38,m}, V. Volkov³³, A. Vollhardt⁴², B. Voneki⁴⁰, A. Vorobyev³¹, V. Vorobyev³⁶, C. Voß⁶⁶, J. A. de Vries⁴³, C. Vázquez Sierra³⁹, R. Waldi⁶⁶, C. Wallace⁵⁰, R. Wallace¹³, J. Walsh²⁴, J. Wang⁶¹, D. R. Ward⁴⁹, H. M. Wark⁵⁴, N. K. Watson⁴⁷, D. Websdale⁵⁵, A. Weiden⁴², M. Whitehead⁴⁰, J. Wicht⁵⁰, G. Wilkinson^{57,40}, M. Wilkinson⁶¹, M. Williams⁴⁰, M. P. Williams⁴⁷, M. Williams⁵⁸, T. Williams⁴⁷, F. F. Wilson⁵¹, J. Wimberley⁶⁰, J. Wishahli¹⁰, W. Wislicki²⁹, M. Witek²⁷, G. Wormser⁷, S. A. Wotton⁴⁹, K. Wraight⁵³, S. Wright⁴⁹, K. Wyllie⁴⁰, Y. Xie⁶⁴, Z. Xing⁶¹, Z. Xu⁴¹, Z. Yang³, H. Yin⁶⁴, J. Yu⁶⁴, X. Yuan³⁶, O. Yushchenko³⁷, K. A. Zarebski⁴⁷, M. Zavertyaev^{11,c}, L. Zhang³, Y. Zhang⁷, Y. Zhang⁶³, A. Zhelezov¹², Y. Zheng⁶³, A. Zhokhov³², X. Zhu³, V. Zhukov⁹, S. Zucchelli¹⁵

Primary affiliations

¹Centro Brasileiro de Pesquisas Físicas (CBPF), Rio de Janeiro 22290-180, Brazil. ²Universidade Federal do Rio de Janeiro (UFRJ), Rio de Janeiro 21941-972, Brazil. ³Center for High Energy Physics, Tsinghua University, Beijing 100084, China. ⁴LAPP, Université Savoie Mont-Blanc, CNRS/IN2P3, Annecy-Le-Vieux 74941, France. ⁵Clermont Université, Université Blaise Pascal, CNRS/IN2P3, LPC, Clermont-Ferrand 63177, France. ⁶CPPM, Aix-Marseille Université, CNRS/IN2P3, Marseille 12388, France. ⁷LAL, Université Paris-Sud, CNRS/IN2P3, Orsay 91898, France. ⁸LPNHE, Université Pierre et Marie Curie, Université Paris Diderot, CNRS/IN2P3, Paris 75252, France. ⁹I. Physikalisches Institut, RWTH Aachen University, Aachen D-52056, Germany. ¹⁰Fakultät Physik, Technische Universität Dortmund, Dortmund D-44221, Germany. ¹¹Max-Planck-Institut für Kernphysik (MPIK), Heidelberg D-69029, Germany. ¹²Physikalisches Institut, Ruprecht-Karls-Universität Heidelberg, Heidelberg D-69120, Germany. ¹³School of Physics, University College Dublin, Dublin 4, Ireland. ¹⁴Sezione INFN di Bari, Bari I-70126, Italy. ¹⁵Sezione INFN di Bologna, Bologna I-40126, Italy. ¹⁶Sezione INFN di Cagliari, Cagliari I-09042, Italy. ¹⁷Sezione INFN di Ferrara, Ferrara I-44100, Italy. ¹⁸Sezione INFN di Firenze, Firenze I-50019, Italy. ¹⁹Laboratori Nazionali dell'INFN di Frascati, Frascati I-00044, Italy. ²⁰Sezione INFN di Genova, Genova I-16146, Italy. ²¹Sezione INFN di Milano Bicocca, Milano I-20133, Italy. ²²Sezione INFN di Milano, Milano I-20133, Italy. ²³Sezione INFN di Padova, Padova I-35131, Italy. ²⁴Sezione INFN di Pisa, Pisa I-56127, Italy. ²⁵Sezione INFN di Roma Tor Vergata, Roma I-00133, Italy. ²⁶Sezione INFN di Roma La Sapienza, Roma I-00185, Italy. ²⁷Henryk Niewodniczanski Institute of Nuclear Physics Polish Academy of Sciences, Kraków PL-31-342, Poland. ²⁸AGH - University of Science and Technology, Faculty of Physics and Applied Computer Science, Kraków PL-30-059, Poland. ²⁹National Center for Nuclear Research (NCBJ), Warsaw PL- 00-681, Poland. ³⁰Horia Hulubei National Institute of Physics and Nuclear Engineering, Bucharest-Magurele 76900, Romania. ³¹Petersburg Nuclear Physics Institute (PNPI), Gatchina RU-188350, Russia. ³²Institute of Theoretical and Experimental Physics (ITEP), Moscow RU-117259, Russia. ³³Institute of Nuclear Physics, Moscow State University (SINP MSU), Moscow 119991, Russia. ³⁴Institute for Nuclear Research of the Russian Academy of Sciences (INR RAN), Moscow RU-117312, Russia. ³⁵Yandex School of Data Analysis, Moscow 119021, Russia. ³⁶Budker Institute of Nuclear Physics (SB RAS) and Novosibirsk State University, Novosibirsk RU-630-090, Russia. ³⁷Institute for High Energy Physics (IHEP), Protvino RU0142281, Russia. ³⁸ICCUB, Universitat de Barcelona, Barcelona E-08028, Spain. ³⁹Universidad de Santiago de Compostela, Santiago de Compostela E-15782, Spain. ⁴⁰European Organization for Nuclear Research (CERN), Geneva CH-1211, Switzerland. ⁴¹Ecole Polytechnique Fédérale de Lausanne (EPFL), Lausanne CH-1015, Switzerland. ⁴²Physik-Institut, Universität Zürich, Zürich CH-8057, Switzerland. ⁴³Nikhef National Institute for Subatomic Physics, Amsterdam NL-1009, The Netherlands. ⁴⁴Nikhef National Institute for Subatomic Physics and VU University Amsterdam, Amsterdam NL-1081, The Netherlands. ⁴⁵NSC Kharkiv Institute of Physics and Technology (NSC KIPT), Kharkiv 61108, Ukraine. ⁴⁶Institute for Nuclear Research of the National Academy of Sciences (KINR), Kyiv 03680, Ukraine. ⁴⁷University of Birmingham, Birmingham B15 2TT, UK.

⁴⁸H.H. Wills Physics Laboratory, University of Bristol, Bristol BS8 1TL, UK. ⁴⁹Cavendish Laboratory, University of Cambridge, Cambridge CB3 0HE, UK. ⁵⁰Department of Physics, University of Warwick, Coventry CV4 7AL, UK. ⁵¹STFC Rutherford Appleton Laboratory, Didcot OX11 0QX, UK. ⁵²School of Physics and Astronomy, University of Edinburgh, Edinburgh EH9 3JZ, UK. ⁵³School of Physics and Astronomy, University of Glasgow, Glasgow G12 8QQ, UK. ⁵⁴Oliver Lodge Laboratory, University of Liverpool, Liverpool L69 7ZE, UK. ⁵⁵Imperial College London, London SW7 2BZ, UK. ⁵⁶School of Physics and Astronomy, University of Manchester, Manchester M13 9PL, UK. ⁵⁷Department of Physics, University of Oxford, Oxford OX1 3RH, UK. ⁵⁸Massachusetts Institute of Technology, Cambridge, Massachusetts 02139, USA. ⁵⁹University of Cincinnati, Cincinnati, Ohio 45221-0011, USA. ⁶⁰University of Maryland, College Park, Maryland 20742, USA. ⁶¹Syracuse University, Syracuse, New York 13244-1130, USA. ⁶²Pontifícia Universidade Católica do Rio de Janeiro (PUC-Rio), Rio de Janeiro 22451-900, Brazil, associated to 2. ⁶³University of Chinese Academy of Sciences, Beijing 100049, China, associated to 3. ⁶⁴Institute of Particle Physics, Central China Normal University, Wuhan, Hubei 430079, China, associated to 3. ⁶⁵Departamento de Física, Universidad Nacional de Colombia, Bogota 21716, Colombia, associated to 8. ⁶⁶Institut für Physik, Universität Rostock, Rostock D-18051, Germany, associated to 12. ⁶⁷National Research Centre Kurchatov Institute, Moscow 123182, Russia, associated to 32. ⁶⁸Instituto de Física Corpuscular (IFIC), Universitat de Valencia-CSIC, Valencia E-46980, Spain, associated to 38. ⁶⁹Van Swinderen Institute, University of Groningen, Groningen 9747 AG, The Netherlands, associated to 43.

Secondary affiliations

^aUniversidade Federal do Triângulo Mineiro (UFMT), Uberaba-MG, Brazil. ^bLaboratoire Leprince-Ringuet, Palaiseau, France. ^cP.N. Lebedev Physical Institute, Russian Academy of Science (LPI RAS), Moscow, Russia. ^dUniversità di Bari, Bari I-70126, Italy. ^eUniversità di Bologna, Bologna I-40126, Italy. ^fUniversità di Cagliari, Cagliari I-09042, Italy. ^gUniversità di Ferrara, Ferrara I-44100, Italy. ^hUniversità di Genova, Genova I-16146, Italy. ⁱUniversità di Milano Bicocca, Milano I-20133, Italy. ^jUniversità di Roma Tor Vergata, Roma I-00133, Italy. ^kUniversità di Roma La Sapienza, Roma I-00185, Italy. ^lAGH - University of Science and Technology, Faculty of Computer Science, Electronics and Telecommunications, Kraków PL-30-059, Poland. ^mLIFAELS, La Salle, Universitat Ramon Llull, Barcelona, Spain. ⁿHanoi University of Science, Hanoi, Vietnam. ^oUniversità di Padova, Padova I-35131, Italy. ^pUniversità di Pisa, Pisa I-56127, Italy. ^qUniversità degli Studi di Milano, Milano I-20133, Italy. ^rUniversità di Urbino, Urbino, Italy. ^sUniversità della Basilicata, Potenza, Italy. ^tScuola Normale Superiore, Pisa, Italy. ^uUniversità di Modena e Reggio Emilia, Modena, Italy. ^vIligan Institute of Technology (IIT), Iligan, Philippines.